

1 **Significant recent warming over the northern Tibetan**  
2 **Plateau from ice core  $\delta^{18}\text{O}$  records**

3

4 **Wenling An<sup>1</sup>, Shugui Hou<sup>1,5\*</sup>, Wangbin Zhang<sup>1</sup>, Yetang Wang<sup>2</sup>, Yaping Liu<sup>3</sup>, Shuangye Wu<sup>1,4</sup>,**  
5 **Hongxi Pang<sup>1</sup>**

6 1 Key Laboratory of Coast and Island development of Ministry of Education, School of  
7 Geographic and Oceanographic Sciences, Nanjing University, Nanjing 210093, China

8 2 College of Population, Resources and Environment, Shandong Normal University, Jinan 250014,  
9 China

10 3 State Key Laboratory of Cryospheric Science, Cold and Arid Regions Environmental and  
11 Engineering Research Institute, Chinese Academy of Sciences, Lanzhou 730000, China

12 4 Geology Department, University of Dayton, Ohio 45469-2364, USA

13 5 CAS Center for Excellence in Tibetan Plateau Earth Sciences, Beijing 100101, China

14 \* Correspondence to: S. Hou (shugui@nju.edu.cn)

15

16

17

18

19

20

21

22

23 **Abstract:** Stable oxygen isotopic records in ice cores provide valuable information about past  
24 temperature, especially for regions with scarce instrumental measurements. This paper presents  
25 the  $\delta^{18}\text{O}$  result of an ice core drilled to bedrock from Mt. Zangser Kangri (ZK), a remote area on  
26 the northern Tibetan Plateau (TP). We reconstructed the temperature series for 1951-2008 from the  
27  $\delta^{18}\text{O}$  records. In addition, we combined the ZK  $\delta^{18}\text{O}$  records with those from three other ice cores  
28 in the northern TP (Muztagata, Puruogangri and Geladaindong) to reconstruct a regional  
29 temperature history for the period 1951-2002 (RTNTP). The RTNTP showed significant warming  
30 at  $0.51\pm 0.07^{\circ}\text{C}(10\text{yr})^{-1}$  since 1970, a higher rate than the trend of instrumental records of the  
31 northern TP ( $0.43\pm 0.08^{\circ}\text{C}(10\text{yr})^{-1}$ ) and the global temperature trend ( $0.27\pm 0.03^{\circ}\text{C}(10\text{yr})^{-1}$ ) at the  
32 same time. In addition, the ZK temperature record, with extra length until 2008, seems to suggest  
33 that the rapid elevation-dependent warming continued for this region during the last decade, when  
34 the mean global temperature showed very little change. This could provide insights into the  
35 behavior of the recent warming hiatus at higher elevations, where instrumental climate records are  
36 lacking.

37

38

39

40

41

42

43

44

## 45 **1. Introduction**

46 With an average elevation over 4000 m a.s.l., the Tibetan Plateau (TP) is the highest and most  
47 extensive highland in the world. In recent decades, it has experienced rapid warming and drastic  
48 environmental changes such as fast glacier retreat and land deterioration (Yao et al., 2012). In  
49 recent years, the global average surface temperature has experienced relatively little change in  
50 recent years (Easterlin and Wehner, 2009), whereas accelerated warming continued on the TP for  
51 the same period of time (Yan and Liu, 2014; Duan and Wu, 2015). However, the rapid warming  
52 trend over the Plateau was established with data from meteorological stations located at relatively  
53 low elevations, and warming trend for higher elevation regions remains uncertain.

54 In addition, spatial biases also exist in the TP temperature records. Most instrumental records  
55 as well as various paleoclimate proxies are located in the eastern and southern Plateau (Thompson  
56 et al., 2000; B. Yang et al., 2014; Herzschuh et al., 2010; Pu et al., 2011). There is generally a lack  
57 of climate data in the northern, and particularly in the northwest TP, where meteorological stations  
58 were sparse, and long-term high-resolution climate records were difficult to obtain because of the  
59 formidable terrain and harsh environment. However, the northern TP (Fig. 1) is a climatologically  
60 important region involving complicated interactions between the mid-latitude westerlies and the  
61 subtropical Asia monsoon circulation. It may serve as a bridge linking the high and low latitude  
62 climatic processes (Y. X. He et al., 2013). It is therefore essential to evaluate the extent and  
63 magnitude of regional climate changes over this region without coverage bias.

64 The ice core  $\delta^{18}\text{O}$  is an important paleoclimate proxy on the TP (Thompson et al., 2000; Qin  
65 et al., 2002), and has been generally considered to be a reliable indicator for past temperatures  
66 (Yao et al., 2006; Joswiak et al., 2010). However, great discrepancies still exist among different

67 temperature reconstructions and instrumental records owing to the distinct geographic locations  
68 and atmospheric circulation conditions (Liu and Chen, 2000; N. Wang et al., 2003; Y. Q. Wang et  
69 al., 2003; Yao et al., 2006). Therefore, it is important to establish more high resolution temperature  
70 records on the TP, particularly over such extensive high elevation regions as the northern TP, in  
71 order to evaluate the warming trends at high elevations in light of the recent warming hiatus. In  
72 this study, we measured the  $\delta^{18}\text{O}$  values in an ice core drilled from the Zangser Kangri (ZK)  
73 glacier on the northern TP, from which temperature changes in the past decades could be  
74 established. The ZK ice core  $\delta^{18}\text{O}$  records made it possible to study the past climate variations  
75 over a relatively inaccessible part of the TP, where instrumental records are very limited. In  
76 addition, we also established the regional climate change history by combining ZK with the  $\delta^{18}\text{O}$   
77 records from other ice cores in the northern TP.

78

## 79 **2 Methodology and Data**

### 80 **2.1 Research area and ice core dating**

81 The ZK glacier is located in the northwest part of the TP, covering an area of 337.98 km<sup>2</sup>  
82 with a volume of 41.70 km<sup>3</sup> (2005 data, Shi, 2008). The snowline is about 5700~5940 m a.s.l.. In  
83 the April of 2009, two ice cores to bedrock (127.7m and 126.7m in length for Core 1 and Core 2  
84 respectively) were recovered from the glacier (34°18'05.8"N, 85°51'14.2"E, 6226 m a.s.l., Fig.1).  
85 The glacier temperature ranged from -15.2°C to -9.2°C, with a mean temperature of -11.7°C,  
86 -12.4°C at 10 m depth and a basal temperature of -9.2°C.

87 These two ice cores were kept frozen and transported to the State Key Laboratory of  
88 Cryospheric Sciences, Cold and Arid Regions Environmental and Engineering Research Institute,

89 Chinese Academy of Sciences for processing. This study was based upon the analysis of Core 1. A  
90 total of 2884 samples were taken from Core 1 at a resolution of 4~6 cm. The outer ~2 cm of each  
91 sample was removed for stable oxygen isotope analysis. The inner portion of the ice core was  
92 collected in pre-cleaned polyethylene sample containers for chemical and dust particle analyses.  
93 Stable oxygen isotope ratio ( $\delta^{18}\text{O}$ ) was determined using a Picarro Wavelength Scanned Cavity  
94 Ring-Down Spectrometer (WS-CRDS, model L2120i). Major cations and anions were analyzed  
95 using a Dionex-600 and ICS-2500 ion chromatograph respectively.

96 In the northern TP, the annual cycle of  $\delta^{18}\text{O}$  along the ice core profile is primarily related to  
97 temperature variations (Araguás-Araguás et al., 1998; Yao et al., 2013). The  $\delta^{18}\text{O}$  compositions in  
98 modern precipitation samples collected at northern TP show marked seasonal patterns with the  
99 high values in summer and low values in winter (Yu et al., 2009). In addition, the major ions (e.g.,  
100  $\text{Mg}^{2+}$  and  $\text{SO}_4^{2-}$ ) also show clear seasonal cycles with high concentrations in winter/spring and  
101 low concentrations in summer (Zheng et al., 2010). They have been used in past studies as  
102 complementary tools in ice core dating in the northern TP (Kang et al., 2007). Therefore, the ZK  
103 ice core was dated by using the seasonality of  $\delta^{18}\text{O}$  in conjunction with the seasonal variations of  
104 major ions, including  $\text{Mg}^{2+}$ ,  $\text{Ca}^{2+}$  and  $\text{SO}_4^{2-}$ , with a reference layer of  $\beta$  activity peak in 1963 (Fig.  
105 2). The core 1 was dated back to 1951 at 16.38 m depth with uncertainty estimated within 1 year  
106 (Fig. 2, Zhang et al., 2016). Based on the dating result and density of the ice core profile, the mean  
107 annual net accumulation rate was estimated to be low for ZK glaciers ( $190 \text{ kg H}_2\text{O m}^{-1} \text{ yr}^{-1}$ ). This  
108 study focused on the  $\delta^{18}\text{O}$  records in the top 16.38 m of the ice core, corresponding to the time  
109 period 1951-2008.

110

## 111 **2.2 Climate data**

112 The ZK glacier is located at a transition zone with shifting influences between the westerlies  
113 and the Indian summer monsoon (Yao et al., 2013). Based on the climate records from the two  
114 nearby meteorological stations, at Gêrzê (32°09', 84°25', 4414.9m a.s.l., 1973-2008) and Xainza  
115 (30°57', 88°38', 4800m a.s.l., 1961-2008) (Fig. 1), the local mean monthly temperature ranges  
116 from -10.8°C in January to 10.7°C in July, with an annual average of 0°C. Precipitation averages  
117 257 mm per year, of which 75% falls between June and September (Fig. S1a).

118 In order to establish the representativeness of the ZK ice core  $\delta^{18}\text{O}$  for the regional climate,  
119 we performed correlation analysis, using Pearson's correlation coefficient ( $r$ ), between the ice core  
120  $\delta^{18}\text{O}$  time series and temperature records from the nearby meteorological stations (Gêrzê and  
121 Xainza), and the instrumental temperature series from a network of meteorological stations in the  
122 northern TP (hereafter, ITNTP). The ITNTP time series was derived from 14 climate stations used  
123 in Guo and Wang (2011), and was extended to 2014 based on the data provided by the Data and  
124 Information Center, China Meteorological Administration. It should be noted that most of the  
125 stations used in ITNTP time series were located on the eastern part of the northern TP with  
126 altitudes ranging from 2767 to 3367 m (Guo and Wang, 2011), whereas this study focused on the  
127 higher (> 5700 m) and more extensive western part of the northern TP (Fig. 1). In addition, spatial  
128 correlations were carried out between ZK  $\delta^{18}\text{O}$  and the CRU 4 gridded temperature reanalysis data  
129 (Mitchell and Jones, 2005) on the KNMI Climate Explorer (<http://climexp.knmi.nl>).

130 In this study, in addition to the ZK series, we also attempted to reconstruct a regional  
131 temperature series by combining ZK with other ice core  $\delta^{18}\text{O}$  records in the northern TP, including  
132 Muztagata (Tian et al., 2006), Puruogangri (Yao et al., 2006), Geladaindong (Kang et al., 2007)

133 and Malan (N. Wang et al., 2003) (Fig. 4 and Table 2). We first examined the consistency of these  
134 ice core records and excluded Malan from the reconstruction because of its drastically different  
135 temporal patterns from the rest of the records. To combine the remaining 4 ice core records, we  
136 derived the  $\delta^{18}\text{O}$  anomalies for each ice core series to eliminate the difference in the absolute  
137 values, and calculated their average (Fig. S2), which was then used to reconstruct the regional  
138 temperature time series.

139

### 140 **3 Results and Discussion**

#### 141 **3.1 The ZK ice core $\delta^{18}\text{O}$ variation and its relationship with regional** 142 **meteorological data**

143 The raw  $\delta^{18}\text{O}$  values throughout the ZK ice core profile from 1951 to 2008 were presented in  
144 Figure 2. For this section, the  $\delta^{18}\text{O}$  values ranged from -17.65‰ at 13.8 m to -3.79‰ at 6.85 m,  
145 with an average value of -10.97‰ (Fig. 2). The  $\delta^{18}\text{O}$  values were relatively low in the 1960s,  
146 followed by an increasing trend from 1970s to the end of the record.

147 Stable oxygen isotope in precipitation could be affected by a variety of environmental factors.  
148 In addition to temperature, the  $\delta^{18}\text{O}$  values in ice cores could also be affected by precipitation  
149 seasonality and amount (Dansgaard, 1964). To exclude possible influence of precipitation, we first  
150 examined whether the seasonal distribution of precipitation experienced any significant changes  
151 during the study period by using the precipitation records from the two nearby stations. Results  
152 showed weak positive trends for the proportion of precipitation in winter and spring, and no  
153 statistically significant trends for the proportions of precipitation in summer and fall (Fig. S1b and  
154 c). This suggests that changes in seasonal distribution of precipitation did not exert a major

155 influence on the  $\delta^{18}\text{O}$  values in ZK ice cores during the period 1961-2008. Besides, we found no  
156 significant correlation between the ZK  $\delta^{18}\text{O}$  record and precipitation amount recorded at the  
157 stations (Table S1). Partial correlation analysis showed this to be true even when annual  
158 temperature was controlled ( $r_{\text{partial}} = 0.01$ ,  $p > 0.1$ ). This suggests that precipitation amount had  
159 little influence on the ZK  $\delta^{18}\text{O}$  values.

160 On the other hand, the ZK  $\delta^{18}\text{O}$  time series showed positive correlation with annual  
161 temperature measured at each of the nearby stations ( $r = 0.31$ ,  $p = 0.07$  for the Gêrzê station;  $r =$   
162  $0.43$ ,  $p = 0.002$  for the Xainza station), the mean annual temperature of the two stations ( $r = 0.34$ ,  
163  $p = 0.01$ ), and ITNTP ( $r = 0.35$ ,  $p = 0.02$ ) (Table 1). Stronger correlation existed between the ZK  
164  $\delta^{18}\text{O}$  and spring (March-May) temperature of the stations (Table 1). Linear regressions led to a  
165 mean  $\delta^{18}\text{O}$ -temperature slope of  $0.85\text{‰ }^{\circ}\text{C}^{-1}$  with values ranging from  $0.67$  to  $0.98\text{‰ }^{\circ}\text{C}^{-1}$  (Table  
166 1). This is consistent with the published  $\delta^{18}\text{O}$ -temperature relationships derived from ice cores  
167 over the northern TP (X. X. Yang et al., 2014).

168 Significant spatial correlation existed between the ZK  $\delta^{18}\text{O}$  series and the CRU gridded  
169 temperature data in the region surrounding the drilling site. The ZK  $\delta^{18}\text{O}$  series showed positive  
170 correlations with annual mean and minimum temperatures for most part of the northern TP (Fig. 3).  
171 The most significant and spatially extensive correlations were found between the ZK  $\delta^{18}\text{O}$  and  
172 spring temperatures (Fig. 3c and d), which were consistent with previous results between the ZK  
173  $\delta^{18}\text{O}$  series and station temperature records (Table 1). The stronger spring temperature signal  
174 recorded in ZK  $\delta^{18}\text{O}$  record may be attributed to the different seasonal moisture sources in this  
175 region. At Shiquanhe and Gêrzê, Yu et al. (2009) found that during the non-monsoon period  
176 (October–June) when local moisture recycling and the westerlies dominate the moisture sources,



177 air temperature correlates more strongly with  $\delta^{18}\text{O}$  in precipitation. On the other hand,  
178 precipitation  $\delta^{18}\text{O}$  in monsoon season could be affected by a variety of factors other than  
179 temperature, including the convection intensity, distance from moisture sources and amount effect  
180 (Y. He et al., 2015; Tang et al., 2015). This could obscure the relationship between  $\delta^{18}\text{O}$  and air  
181 temperatures (Joswiak et al., 2013). In addition, previous studies in the central Himalayas found  
182 that high elevation areas ( $> 3000\text{m.a.s.l.}$ ) can receive up to 40% of their annual precipitation during  
183 cold season because of terrain locked low pressure systems and orographically forced precipitation  
184 (Lang and Barros, 2004), a much higher percentage than that of surrounding low altitude areas of  
185 the same region (Pang et al., 2014). Therefore, the ZK ice core (located at 6226 m a.s.l.) could  
186 have had more cold-season (non-monsoonal) precipitation than that indicated by nearby  
187 meteorological stations, located at much lower elevations. Both factors could result in a stronger  
188 signal of spring temperature in the ZK ice core  $\delta^{18}\text{O}$  record.

189

### 190 **3.2 Regional temperature reconstruction**

191 Detailed comparisons were made between the ZK  $\delta^{18}\text{O}$  and the  $\delta^{18}\text{O}$  time series of four  
192 nearby ice cores, including Muztagata, Puruogangri, Geladaindong and Malan (Fig. 4 and Table 2).  
193 The cooling around 1960s was present in all ice cores, and this was consistent with the observed  
194 cold period during this time over the entire TP (Liu and Chen, 2000). Moreover, the significant  
195 increasing trend from 1970s to present was observed in all except Malan ice core  $\delta^{18}\text{O}$  series. We  
196 calculated the Pearson correlation coefficients among these ice core  $\delta^{18}\text{O}$  series (Table 3). The  
197 results showed weak correlations between the annual values of these series. This lack of  
198 correlation could result from the differences in location, elevation and hence local climates. It

199 could also arise from uncertainties in ice core dating. In order to reduce the impact of dating  
200 uncertainties, we used the 5 year running averages instead of annual values, and these series  
201 showed much stronger correlations, suggesting possible common regional climate patterns  
202 preserved in these ice core series. This coherence is important when we use the average of  
203 multiple sites to develop a regional composite.

204 In contrast to the rest of the ice cores, the Malan  $\delta^{18}\text{O}$  record showed a cooling trend since  
205 1970s (Fig. 4e). Such continuous low level of  $\delta^{18}\text{O}$  could be caused by the change of local climate  
206 conditions (Y. Q. Wang et al., 2003), but could also result from post-depositional processes on the  
207 chemical profiles, such as summer melting, evaporation and condensation, all of which could  
208 modify the relationship between ice core  $\delta^{18}\text{O}$  and temperature (Hou et al., 2006). Furthermore,  
209 the correlation analysis showed that the Malan time series was negatively correlated with other  
210 four time series, and the negative relationships were more significant after 5 year running  
211 averaging (Table 3). Therefore, we excluded the Malan record from further analysis.

212 Moreover, the correlations between Geladaindong and three other ice cores, i.e. ZK,  
213 Muztagata, Puruogangri were relatively low even after 5 year running averages (Table 3). The lack  
214 of correlation could be attributed to its local climate conditions (Table 3), such as the influence of  
215 local convective vapor due to its more northern location (Kang et al., 2007). However, the ice  
216 cores of ZK, Muztagata, Puruogangri and Geladaindong shared similar patterns of  $\delta^{18}\text{O}$  variations,  
217 especially their increasing trends since 1970s (Fig. 4). Moreover, regional composite with  
218 Geladaindong records correlates very strongly with that without Geladaindong ( $r = 0.95$ ,  
219 1951-2002,  $p < 0.0001$ ), and two series showed very similar temporal patterns (Fig. S2). Therefore,  
220 we decided to include the Geladaindong ice core  $\delta^{18}\text{O}$ , so that the final regional reconstruction

221 could have larger spatial coverage to better represent the regional climate of the northern TP. The  
222 regional temperature series was reconstructed for 1951-2002, the common period covered by the  
223 four ice core  $\delta^{18}\text{O}$  records. Meanwhile, a temperature reconstruction based solely on ZK ice core  
224  $\delta^{18}\text{O}$  record was constructed for 1951-2008 to investigate the temperature variations since the late  
225 1990s.

226 Before establishing the temperature reconstructions, it was necessary to derive the  
227  $\delta^{18}\text{O}$ -temperature relationship to understand the magnitude of the temperature variation over the  
228 northern TP. Yu et al. (2009) calculated the isotope sensitivity between monthly mean  $\delta^{18}\text{O}$  values  
229 in precipitation and the monthly mean temperatures at Gêrzê and Shiquanhe (Fig. 1) as 0.33 and  
230  $0.37\text{‰ }^{\circ}\text{C}^{-1}$  respectively. State of the art atmospheric models with integrated water isotopes  
231 modeling suggested an average isotope sensitivity of  $0.53\text{‰ }^{\circ}\text{C}^{-1}$  for the present-day precipitation  
232 falling at the grid where the ZK core was recovered (Risi et al., 2010). Tian et al. (2006) used the  
233 range of 0.6 to  $0.7\text{‰ }^{\circ}\text{C}^{-1}$  to convert the  $\delta^{18}\text{O}$  values to temperature for the Muztagata ice core.  
234 The isotope sensitivity usually increases with elevation as indicated by Rayleigh-type equilibrium  
235 fractionation model (Rowley et al., 2001). Kang et al. (2007) obtained  $1.40\text{‰ }^{\circ}\text{C}^{-1}$   
236  $\delta^{18}\text{O}$ -temperature relationship from the linear regression between the 5 year running average of  
237 Geladaindong  $\delta^{18}\text{O}$  records and regional instrumental temperature records. In our study, the  
238 strongest correlation was found between the 5 year running average of the regional  $\delta^{18}\text{O}$  record  
239 and ITNTP ( $r = 0.89$ ,  $p < 0.001$ ) (Fig. S3). The ZK  $\delta^{18}\text{O}$  correlates most strongly with the 5 year  
240 running average of the mean temperature from two nearby stations (Gêrzê and Xainza,  $r = 0.60$ ,  $p$   
241  $< 0.001$ ) (Table 1). Based on these significant relationships, the isotope sensitivities were  
242 determined as  $1.46\text{‰ }^{\circ}\text{C}^{-1}$  for the regional  $\delta^{18}\text{O}$  series and  $1.18\text{‰ }^{\circ}\text{C}^{-1}$  for ZK  $\delta^{18}\text{O}$  series, and

243 were used to reconstruct regional temperature series for the northern TP (RTNTP) and the ZK  
244 temperature series respectively. Additional analysis showed that as isotope sensitivity value  
245 increases, the response of decadal warming rate decreases, especially for the isotope sensitivity  
246 values greater than 1.0 (Fig. S4).

247 The reconstructed regional temperature for the northern TP (RTNTP) was presented in Figure  
248 5a together with the temperature reconstruction for the ZK ice core (Fig. 5b), ITNTP (Fig. 5c) and  
249 the global temperature series (Fig. 5d) for comparison. We first compared the RTNTP with the  
250 ITNTP, and found strong correlation between the two temperature series ( $r = 0.65$ ,  $p < 0.001$ ).  
251 Spatially, significant correlations also existed between the CRU gridded surface temperatures and  
252 the ITNTP ( $r = 0.50$  to  $0.60$ ,  $n = 42$ ,  $p < 0.01$ ), as well as between CRU and the RTNTP ( $r = 0.40$   
253 to  $0.60$ ,  $n = 52$ ,  $p < 0.01$ ) over a large region (Fig. 6). The study area had the strongest correlations  
254 ( $r > 0.50$ ,  $p < 0.01$ ). This suggested that the regional reconstruction adequately captured  
255 temperature variation on the northern TP.

256

### 257 **3.3 Recent rapid warming trend over the northern TP**

258 The regional reconstruction was compared with the global annual temperature series (Fig. 5d)  
259 and the ITNTP (Fig. 5c) in order to investigate the recent warming trend since 1970s. LOESS  
260 regression was used to smooth the data and estimate the general trend. The reconstruction captured  
261 the cooling period during 1960s, as well as the prominent warming since the 1970s to the end of  
262 the record, with the highest rate of increase in the late 1990s (Fig. 5). For the period from 1970 to  
263 2002, the RTNTP showed more rapid warming trend at the rate of  $0.51 \pm 0.07^\circ\text{C}(10\text{yr})^{-1}$  than that of  
264 the global temperature ( $0.27 \pm 0.03^\circ\text{C}(10\text{yr})^{-1}$ ). The RTNTP rate was also higher than the ITNTP

265 rate of increase at  $0.43\pm 0.08^{\circ}\text{C}(10\text{yr})^{-1}$  for the same time period. From 1990 to 2002, the warming  
266 accelerated on the northern TP with rates of temperature increase at  $0.95\pm 0.21^{\circ}\text{C}(10\text{yr})^{-1}$  for the  
267 RTNTP and  $0.90\pm 0.29^{\circ}\text{C}(10\text{yr})^{-1}$  for the ITNTP, much higher than the warming rate of the global  
268 temperature ( $0.37\pm 0.13^{\circ}\text{C}(10\text{yr})^{-1}$ ). These results seemed to indicate enhanced warming at the  
269 high elevation regions on the northern TP.

270 Since the late 1990s, the global temperature showed very little change and even decreasing  
271 trend since 2005 (Fig. 5d). The relatively flat warming trend was also recorded in the ITNTP (Fig.  
272 5b). However, the ZK series revealed a continued warming trend in recent years after a brief pause  
273 during the early 2000s (Fig. 5b). We calculated mean decadal annual temperature change based on  
274 the LOESS regression model for all three time series (Fig. 7). For both the global temperature and  
275 ITNTP series, the highest average warming rates occurred during 1990s, and then decreased  
276 significantly since 1999 (Fig. 7c and d). The reduction of warming rate in the ITNTP series was  
277 consistent with results by Duan and Xiao (2015), who found weaker warming trend during the  
278 period 1998-2013 in the northern TP based on the instrumental temperature records. However, the  
279 rates of increase remained high for the temperature records in the ZK series since 1999 (Fig. 7b),  
280 in contrast to the slowdown of climate warming observed for the global mean and ITNTP  
281 temperature records since 1999 (Fig. 7d). The persistent high warming rates derived from our  
282 regional reconstructions seem to suggest that the elevation-dependent warming is still evident over  
283 the high elevations of the northern TP despite the reduced warming rates observed at lower  
284 stations in ITNTP (Fig. S5).

285 The persistent rapid warming in the northern TP could have been caused by the regional  
286 radiative and energy budget changes (K. Yang et al., 2014; Yan and Liu, 2014; Duan and Xiao,

287 2015). Many studies show that the snow/ice-albedo feedback is an important mechanism for  
288 enhanced warming at high elevation regions (Liu and Chen, 2000; Pepin and Lundquist, 2008;  
289 Rangwala and Miller, 2012). Ghatak et al. (2014) found that the surface albedo decreases more at  
290 higher elevations than lower elevations over the TP in recent years. Qu et al. (2013) observed a  
291 decreasing trend for the snow/ice albedo at the Nyainquentanglha glacier region, central TP, for  
292 the period 2000 to 2010. It has been found that the glacier albedo for the nine glaciers in western  
293 China has decreased during the period 2000-2011, especially for the central TP (J. Wang et al.,  
294 2014). For example, the glacial albedo of Dongkemadi and Puruogangri glaciers decreased at a  
295 rate of 0.0043-0.0059 yr<sup>-1</sup> and 0.001-0.004 yr<sup>-1</sup> respectively. Reduced surface albedo increases the  
296 surface absorption of solar radiation, and may have contributed to the continued warming over the  
297 high elevation regions of the northern TP. Further research is needed to identify and quantify the  
298 exact mechanisms accounting for the temperature variations over the Plateau.

299

## 300 **4 Conclusions**

301 This study presented a  $\delta^{18}\text{O}$  time series of the ZK ice core from the northern TP, based on  
302 which a temperature record was reconstructed for the period 1951-2008. Moreover, by combining  
303 the ZK  $\delta^{18}\text{O}$  with three other ice cores from the northern TP, a regional temperature history was  
304 established from 1951 to 2002. These temperature reconstructions captured the rapid warming  
305 trend since 1970, and showed continued warming since 1999 at much higher rates than those of  
306 the global average temperature and the instrumental temperature records for the northern TP.

307 Possible explanations for this continued warming might lie in the regional radiative and  
308 energy changes at higher elevations over the northern TP. However, the exact physical

309 mechanisms responsible for the consistently significant warming at higher elevations remain  
310 unclear, partly due to the scarcity of available observations. Further studies are needed to  
311 understand the specific characteristics of this warming trend on the TP, as well as the response  
312 mechanisms of high elevations regions to global changes.

313

## 314 **Acknowledgments**

315 Thanks are due to many scientists, technicians, graduate students and porters for their hard work in  
316 the field. We would also like to thank Hao Xu, Yaju Li, Chaomin Wang, Hao Hou, Rong Hua,  
317 Jing He and Yanying Tang for their help in the laboratories. This work was supported by the  
318 Natural Science Foundation of China (41330526, 41171052 and 41321062), and the Chinese  
319 Academy of Sciences (XDB03030101-4).

320

321

322

323

324

325

326

327

328

329

330

331 **References**

- 332 Araguás-Araguás, L., Froehlich, K., and Rozanski, K.: Stable isotopic composition of precipitation  
333 over southeast Asia, *J. Geophys. Res.*, 103(D22), 28721–28742, doi: 10.1029/98JD02582,  
334 1998.
- 335 Dansgaard, W.: Stable isotopes in precipitation, *Tellus*, 16(4), 436–468,  
336 doi:10.1111/j.2153-3490.1964.tb00181.x, 1964.
- 337 Duan, A. M. and Xiao, Z. X.: Does the climate warming hiatus exist over the Tibetan Plateau?,  
338 *Scientific Reports*, 5, 13711, doi:10.1038/srep13711, 2015.
- 339 Easterling, D. R. and Wehner M. F.: Is the climate warming or cooling? *Geophys. Res. Lett.*, 36,  
340 L08706, doi:10.1029/2009GL037810, 2009.
- 341 Ghatak, D., Sinsky, E., and Miller, J.: Role of snow-albedo feedback in higher elevation warming  
342 over the Himalayas, Tibetan Plateau and Central Asia, *Environ. Res. Lett.*, 9, 114008,  
343 doi:10.1088/1748-9326/9/11/114008, 2014.
- 344 Guo, D. L. and Wang, H. J.: The significant climate warming in the northern Tibetan Plateau and  
345 its possible causes, *Int. J. Climatol.*, 32, 1775–1781, doi: 10.1002/joc.2388, 2011.
- 346 He, Y. X., Zhao, C., Wang, Z., Wang, H. Y., Song, M., Liu, W. G., and Liu, Z. H.: Late Holocene  
347 coupled moisture and temperature changes on the northern Tibetan Plateau. *Quaternary Sci.*  
348 *Rev.*, 80, 47-57, doi:10.1016/j.quascirev.2013.08.017, 2013.
- 349 He, Y., Risi, C., Gao, J., Masson-Delmotte, V., Yao, T. D., Lai, C. T., Ding, Y. J., Worden, J.,  
350 Frankenberg, C., Chepfer, H., and Cesana, G.: Impact of atmospheric convection on south  
351 Tibet summer precipitation isotopologue composition using a combination of in  
352 situ measurements, satellite data, and atmospheric general circulation modeling, *J. Geophys.*



353 Res., 120, 3852–3871, doi:10.1002/2014JD022180, 2015.

354 Herzs Schuh, U., Mischke, H. J., S., Zhang, C. J., and Böhner, J.: A modern pollen-climate  
355 calibration set based on lake sediments from the Tibetan Plateau and its application to a Late  
356 Quaternary pollen record from the Qilian Mountains, *J. Biogeogr.*, 37(4), 752–766,  
357 doi:10.1111/j.1365-2699.2009.02245.x, 2010.

358 Hou, S. G., Ren, J. W., and Qin, D. H.: Modification of three ice-core  $\delta^{18}\text{O}$  records from an area of  
359 high melt, *Ann. Glaciol.*, 43, 172–176, doi: 10.3189/172756406781812140, 2006.

360 Joswiak, D. R., Yao, T., Wu, G., Tian, L., and Xu, B.: Ice-core evidence of westerly and monsoon  
361 moisture contributions in the central Tibetan Plateau, *J. Glaciol.*, 59, 56–66,  
362 doi:10.3189/2013JoG12J035, 2013.

363 Joswiak, D. R., Yao, T., Wu, G., Xu, B., and Zheng, W.: A 70-yr record of oxygen-18 variability in  
364 an ice core from the Tanggula Mountains, central Tibetan Plateau, *Clim. Past*, 6, 219–227, doi:  
365 10.5194/cp-6-219-2010, 2010.

366 Kang, S. C., Zhang, Y. J., Qin, D. H., Ren, J. W., Zhang, Q. G., Bjorn, G., and Mayewski, P. A.:  
367 Recent temperature increase recorded in an ice core in the source region of Yangtze River,  
368 *Chin. Sci. Bull.*, 52(6), 825–831, doi: 10.1007/s11434-007-0140-1, 2007.

369 Lang, T. J. and Barros, A. P.: Winter storms in the central Himalayas, *J. Meteorol. Soc. Jpn.*, 82,  
370 829–844, doi: 10.2151/jmsj.2004.829, 2004.

371 Liu, X. D. and Chen, B. D.: Climatic warming in the Tibetan Plateau during recent decad  
372 es, *Int. J. Climatol.*, 20, 1729–1742, doi:10.1002/1097-0088(20001130)20:14<1729::AID  
373 -25JOC556>3.0.CO;2-Y, 2000.

374 Mitchell, T. D. and Jones, P. D.: An improved method of constructing a database of monthly

375 climate observations and associated high-resolution grids, *Int. J. Climatol.*, 25(6), 693–712,  
376 doi: 10.1002/joc.1181, 2005.

377 Pang, H., Hou, S., Kaspari, S., and Mayewski, P. A.: Influence of regional precipitation patterns on  
378 stable isotopes in ice cores from the central Himalayas, *The Cryosphere*, 8, 289-301,  
379 doi:10.5194/tc-8-289-2014, 2014.

380 Pepin, N. and Lundquist, J.: Temperature trends at high elevations: patterns across the globe,  
381 *Geophys. Res. Lett.*, 35, L14701, doi: 10.1029/2008GL034026, 2008.

382 Pu, Y., Zhang, H. C., Wang, Y. L., Lei, G. L., Nace, T., and Zhang, S. P.: Climatic and  
383 environmental implications from n-alkanes in glacially eroded lake sediments in Tibetan  
384 Plateau: An example from Ximen Co, *Chin. Sci. Bull.*, 56(14), 1503–1510, doi:  
385 10.1007/s11434-011-4454-7, 2011.

386 Qin, D. H., Hou, S. G., Zhang, D. Q., Ren J. W., and Kang, S. C.: Preliminary results from the  
387 chemical records of an 80.4 m ice core recovered from East Rongbuk Glacier, Qomolangma  
388 (Mount Everest), *Ann. Glaciol.*, 35, 278-84, doi: 10.3189/172756402781816799, 2002.

389 Qu, B.: Albedo changing and its impact factors in the glacier area of Mt. Nyainquentanglha region,  
390 Beijing, University of Chinese Academy of Sciences, 35-36, 2013.

391 Rangwala, I. and Miller, J.: Climate change in mountains: a review of elevation dependent  
392 warming and its possible causes, *Clim. Change*, 114, 527–47, doi:  
393 10.1007/s10584-012-0419-3, 2012.

394 Risi, C., Bony, S., Vimeux, F., and Jouzel, J.: Water-stable isotopes in the LMDZ4 general  
395 circulation model: Model evaluation for present - day and past climates and applications to  
396 climatic interpretations of tropical isotopic records, *J. Geophys. Res.*, 115, D12118, doi:

397 10.1029/2009JD013255, 2010.

398 Rowley, D. B., Pierrehumbert, R. T., and Currie, B. S.: A new approach to stable isotope-based  
399 paleoaltimetry: implications for paleoaltimetry and paleohypsometry of the High Himalaya  
400 since the Late Miocene, *Earth Planet. Sci. Lett.*, 188, 253-268, doi:  
401 10.1016/S0012-821X(01)00324-7, 2001.

402 Shi, Y. F.: *Concise Glacier Inventory of China*, Shanghai Science Press, 2008.

403 Thompson, L. G., Yao, T., Mosley-Thompson, E., Davis, M. E., Henderson, K. A., and Lin, P. N.:  
404 A high-resolution millennial record of the South Asian monsoon from Himalayan ice cores,  
405 *Science*, 289, 1916-1919, doi: 10.1126/science.289.5486.1916, 2000.

406 Tang, Y., Pang, H., Zhang, W., Li, Y., Wu, S., and Hou, S.: Effects of changes in moisture source  
407 and the upstream rainout isotopes in precipitation — a case study in Nanjing, East China,  
408 *Hydrol. Earth Syst. Sci.*, 19, 4293-4306, doi:10.5194/hess-19-4293-2015, 2015.

409 Tian, L. D., Yao, T. D., Li, Z., MacClune, K., Wu, G. J., Xu, B. Q., Li, Y. F., Lu, A. X., and Shen, Y.  
410 P.: Recent rapid warming trend revealed from the isotopic record in Muztagata ice core,  
411 eastern Pamirs, *J. Geophys. Res.*, 111, D13103, doi: 10.1029/2005JD006249, 2006.

412 Wang Y. Q., Pu, J. C., Zhang, Y. L., and Sun, W. Z.: Characteristic of present warming change  
413 recorded in Malan ice core, central Tibetan Plateau, *J. Glaciol. Geocryol.*, 25(2), 130-134,  
414 2003 (in Chinese, with English abstracts).

415 Wang, J., Ye, B. S., Cui, Y. H., He, X. B., and Yang, G. J.: Spatial and temporal variations of  
416 albedo on nine glaciers in western China from 2000 to 2011, *Hydrol. Process*, 28(9),  
417 3454-3465, doi: 10.1002/hyp.9883, 2014.

418 Wang, N., Yao, T. D., Pu, J. C., Zhang, Y. L., Sun, W. Z., and Wang, Y. Q.: Variations in air

419 temperature during the last 100 years revealed by  $\delta^{18}\text{O}$  in the Malan ice core from the Tibetan  
420 plateau, *Chin. Sci. Bull.*, 48(19), 2134-2238, doi: 10.1360/02wd0539, 2003.

421 Yan, L. B. and Liu, X. D.: Has Climatic Warming over the Tibetan Plateau Paused or Continued in  
422 Recent Years? *J. Earth Ocean Atmos. Sci.*, 1(1), 13-28, 2014.

423 Yang, B., Qin, C., Wang, J. L., He, M. H., Melvin, T. M., Osborn, T. J., and Briffa, K. R.: A  
424 3,500-year tree-ring record of annual precipitation on the northeastern Tibetan Plateau, *P.  
425 Natl. Acad. Sci. USA*, 111(8), 2903-2908, doi: 10.1073/pnas.1319238111, 2014.

426 Yang, K., Wu, H., Qin, J., Lin, C. G., Tang, W. J., and Chen, Y. Y.: Recent climate changes over the  
427 Tibetan Plateau and their impacts on energy and water cycle: A review, *Global Planet.  
428 Change*, 112, 79–91, doi: 10.1016/j.gloplacha.2013.12.001, 2014.

429 Yang, X. X., Yao, T. D., Joswiak, D., and Yao, P.: Integration of Tibetan Plateau ice-core  
430 temperature records and the influence of atmospheric circulation on isotopic signals in the  
431 past century, *Quaternary Res.*, 81(3), 520-530, doi:10.1016/j.yqres.2014.01.006, 2014.

432 Yao, T. D., Guo, X. J., Lonnie, T., Duan, K. Q., Wang, N. L., Pu, J. C., Xu, B. Q., Yang, X. X., and  
433 Sun, W. Z.:  $\delta^{18}\text{O}$  record and temperature change over the past 100 years in ice cores on the  
434 Tibetan Plateau, *Sci. China Ser. A*, 49(1), 1-9, doi: 10.1007/s11430-004-5096-2, 2006.

435 Yao, T. D., Masson-Delmotte, V., Gao, J., Yu, W. S., Yang, X. X., Risi, C., Sturm, C., Werner, M.,  
436 Zhao, H. B., He, Y., Ren, W., Tian, L. D., Shi, C. M., and Hou, S. G.: A review of climatic  
437 controls on  $\delta^{18}\text{O}$  in precipitation over the Tibetan Plateau: Observations and simulations, *Rev.  
438 Geophys.*, 51(4), 525-548, doi:10.1002/rog.20023, 2013.

439 Yao, T. D., Thompson, L., Yang, W., Yu, W. S., Gao, Y., Guo, X. J., Yang, X. X., Duan, K. Q.,  
440 Zhao, H. B., Baiqing Xu, B. Q., Pu, J. C., Anxin Lu, A. X., Xiang, Y., Kattel D. B., and

441 Joswiak, D.: Different glacier status with atmospheric circulations in Tibetan Plateau and  
442 surroundings, *Nature Clim. Change*, 2, 663-667, doi:10.1038/nclimate1580, 2012.

443 Yu, W. S., Ma, Y. M., Sun, W. Z., and Wang, Y.: Climatic significance of  $\delta^{18}\text{O}$  records from  
444 precipitation on the western Tibetan Plateau, *Chinese Sci. Bull.*, 54, 2732-2741, doi:  
445 10.1007/s11434-009-0495-6, 2009.

446 Zhang, W. B., Hou, S. G., An, W. L., Zhou, L. Y., and Pang, H. X.: Variations of atmospheric dust  
447 loading since 1951 AD recorded in an ice core from the North Tibet Plateau, *Ann. Glaciol.*,  
448 57(71), doi: 10.3189/2016AoG71A559, 2016

449 Zheng, W., Yao, T. D., Joswiak, D. R., Xu, B. Q., Wang, N. L., and Zhao, H. B.: Major ions  
450 composition records from a shallow ice core on Mt. Tanggula in the central Qinghai-Tibetan  
451 Plateau, *Atmos. Res.*, 97(1-2), 70-79, doi:10.1016/j.atmosres.2010.03.008, 2010.

452

453

454

455

456

457

458

459

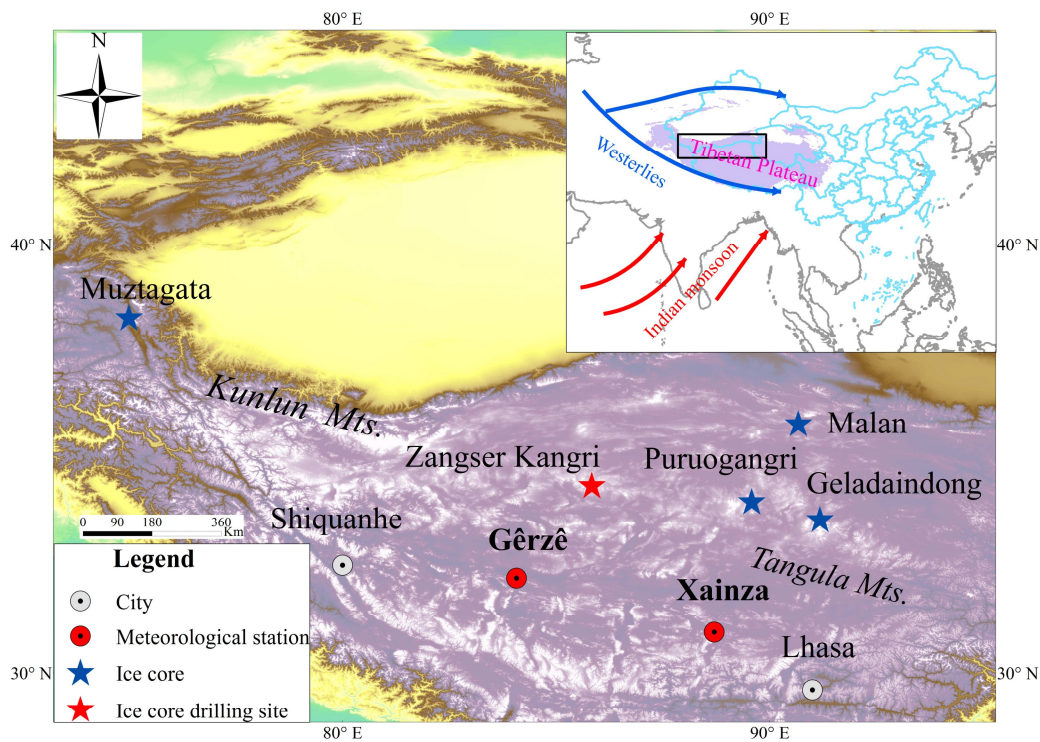
460

461

462

463 **Figures**

464 Figure 1. Location of the ice core drilling site of ZK, two nearby meteorological station sites,  
465 and the location of other ice cores described in the text: Muztagata (Tian et al., 2006),  
466 Puruogangri (Yao et al., 2006), Geladaindong (Kang et al., 2007) and Malan (Wang et al.,  
467 2003) over the northern TP. The inset shows the relative location of the northern TP to the  
468 entire TP. The black rectangle indicates the study area. Red and blue arrows represent the  
469 circulation patterns for the study region. Red arrows indicate the direction of the Indian  
470 monsoon (near surface) in summer, and blue arrows indicate the dominant westerlies (mid to  
471 upper troposphere) in winter.



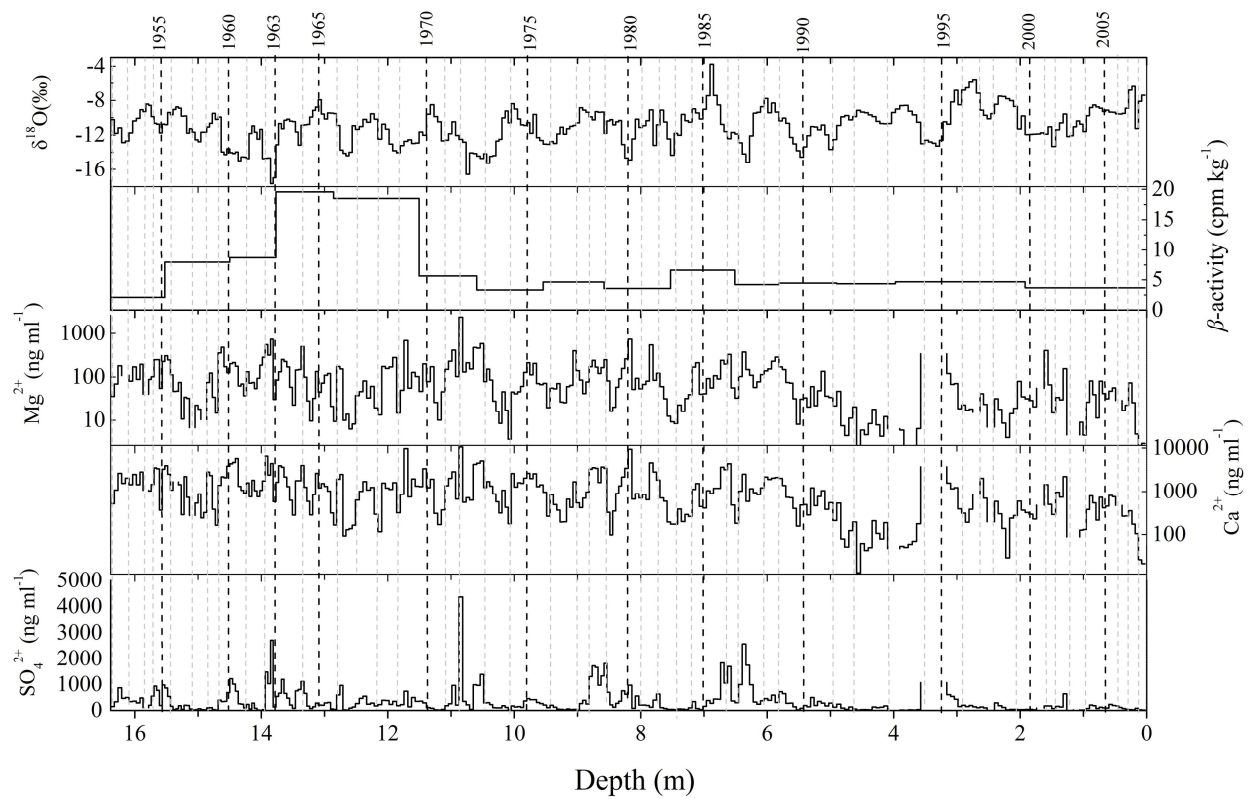
472

473 Figure 2. Variations of  $\delta^{18}\text{O}$  in the ZK ice core and other data used for dating, including beta

474 activity and major ion concentrations. We calculated the logarithm to the base 10 for the

475 concentrations of the  $\text{Ca}^{2+}$  and  $\text{Mg}^{2+}$  to facilitate dating.

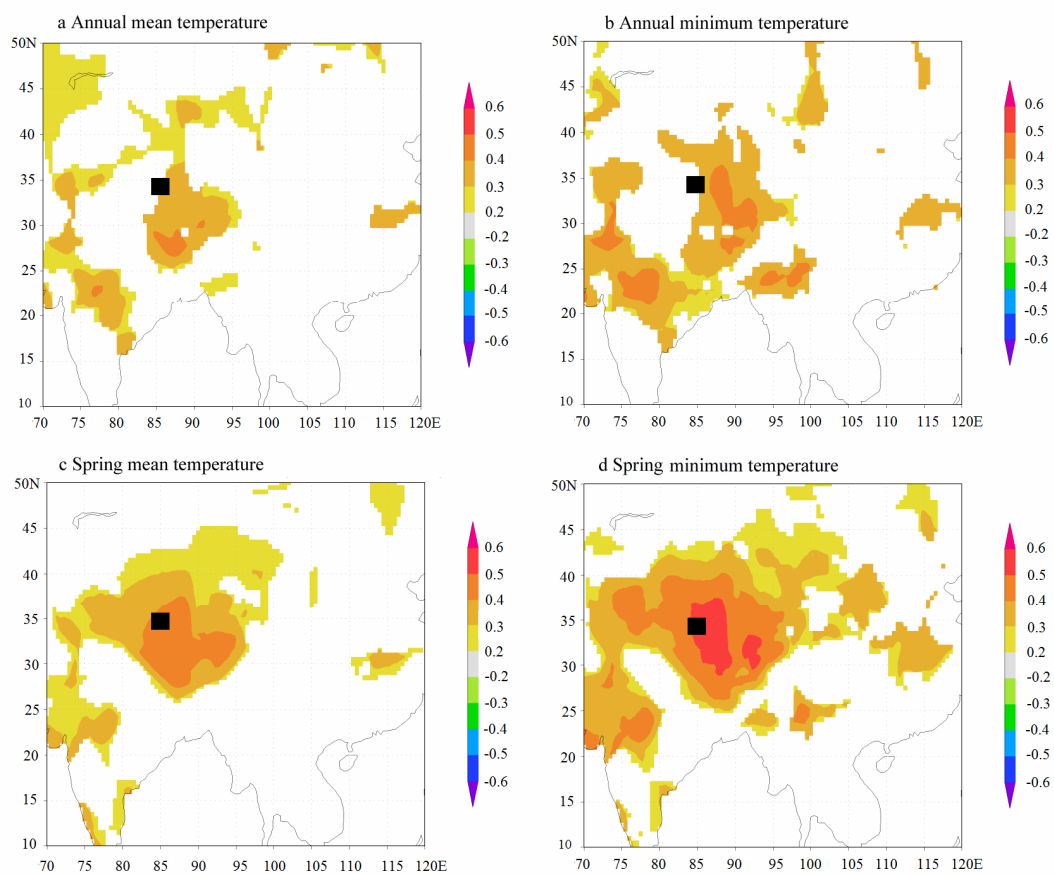
476



477

478 Figure 3. Spatial correlations of ZK ice core  $\delta^{18}\text{O}$  record with CRU-gridded (Mitchell and Jones,  
479 2005) annual mean temperature (a), annual minimum temperature (b), spring mean  
480 temperature (c), and spring minimum temperature (d) for the period 1951-2008. Only  
481 correlation coefficients significant at  $p < 0.01$  are shown. The black rectangle indicates the  
482 ZK ice core site.

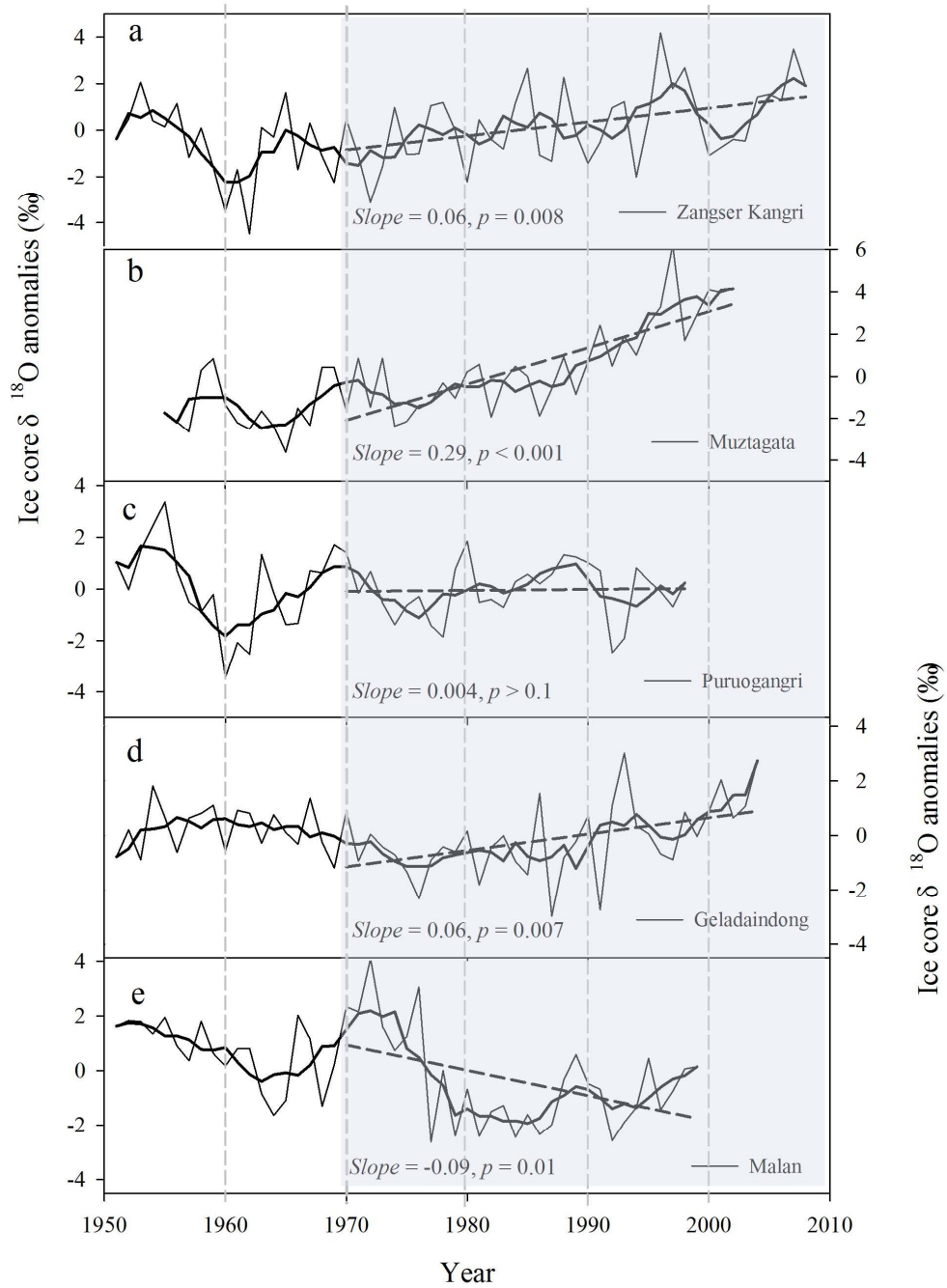
483



484



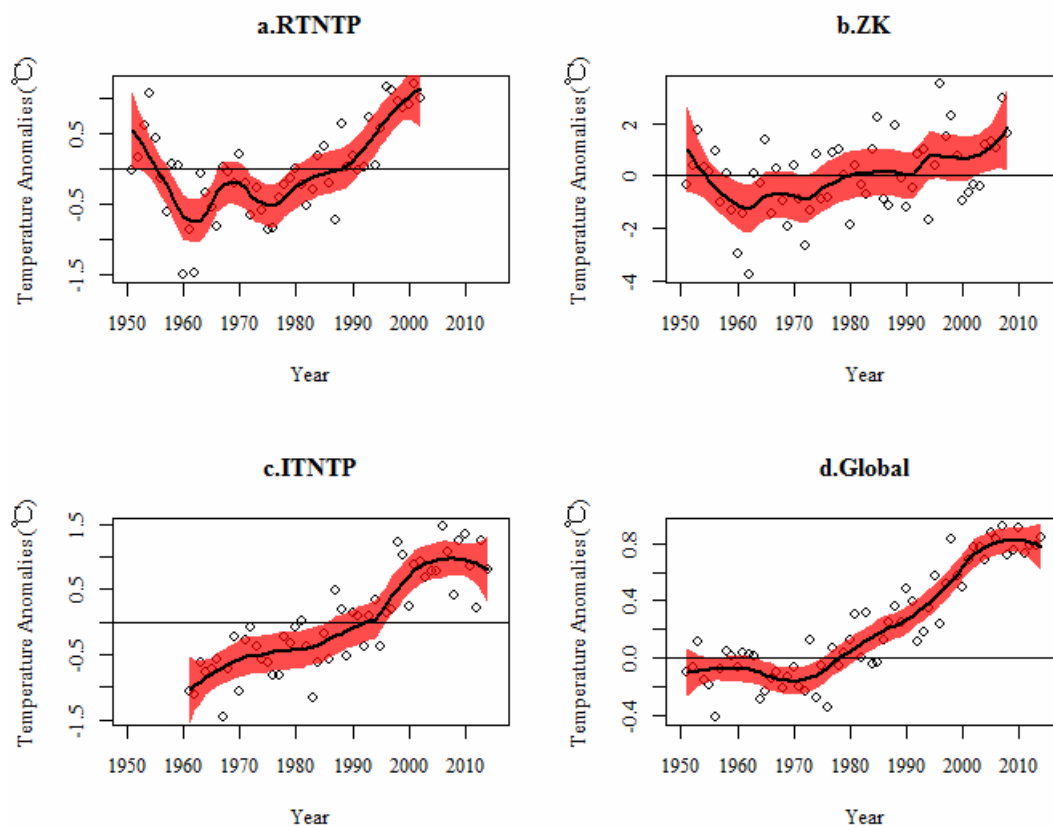
485 Figure 4. Comparisons of the anomalies of  $\delta^{18}\text{O}$  records in the ZK ice core (a) with  $\delta^{18}\text{O}$  records  
 486 from Muztagata (b), Puruogangri (c), Geladaindong (d) and Malan ice cores (e). Thin lines  
 487 represent annual values, thick lines the 5-year running averages, and the dotted lines the  
 488 linear trends since 1970.



489

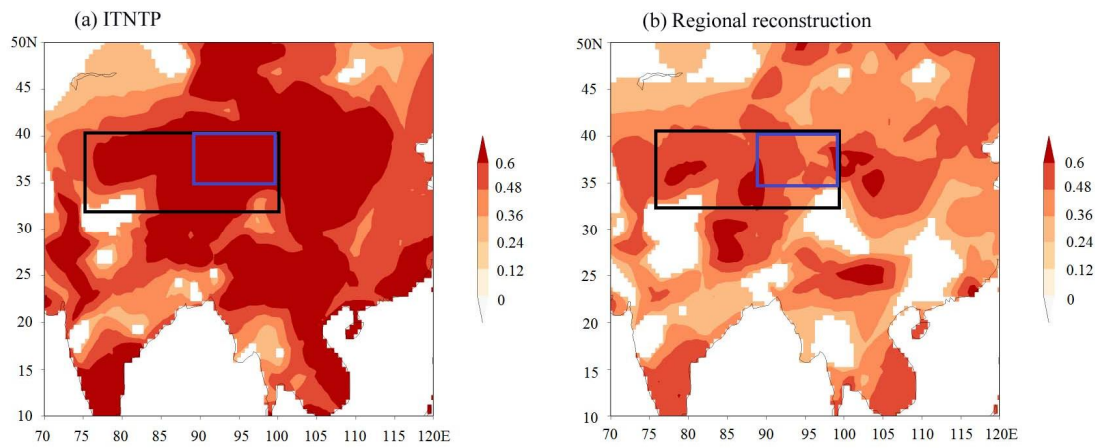
490

491 Figure 5. The reconstructed regional temperature series for northern Tibetan Plateau (RTNTP)  
492 from ZK, Muztagata, Puruogangri and Geladaindong ice core  $\delta^{18}\text{O}$  records (a), the  
493 reconstructed temperature series from ZK ice core  $\delta^{18}\text{O}$  record (b), the instrumental  
494 temperature record for the northern TP (ITNTP) (c), and global average temperature (d).  
495 Black trend lines were estimated using the non-parametric LOESS regression technique with  
496 a span of 0.4; the dots indicate the raw values of corresponding temperature series; shading  
497 represents the 95% confidence intervals of the estimated trends.



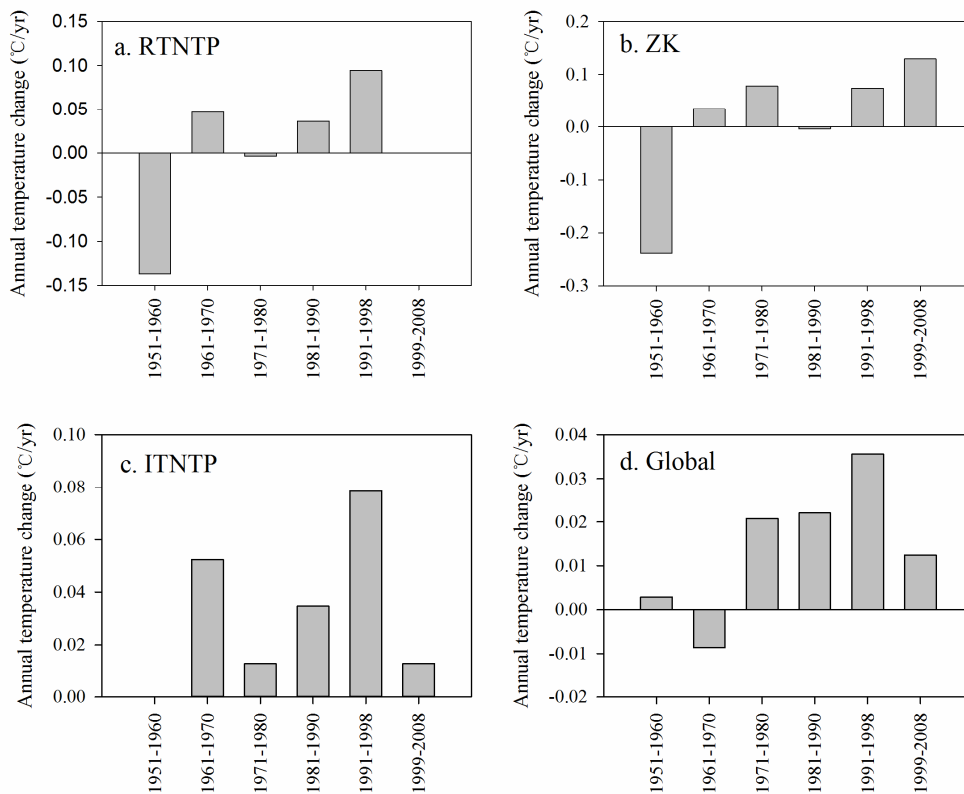
498  
499  
500  
501  
502

503 Figure 6. Spatial correlations ( $r$  values in color,  $p < 0.01$ ) between the gridded annual mean  
504 temperature data (the CRU 4 temperature time series,  $0.5^\circ \times 0.5^\circ$  resolution, Mitchell and  
505 Jones, 2005) and the instrumental temperature record of the northern TP (ITNTP) (Guo and  
506 Wang, 2011) for the period 1961-2002 (a), and the regional temperature reconstruction series  
507 for the period 1961-2002 (b). The black rectangle indicates the study area and the blue  
508 rectangle indicates the region covered by ITNTP.  
509



510

511 Figure 7. Decadal mean annual change rates for the regional temperature reconstruction series for  
 512 northern TP (RTNTP) (a), the temperature reconstruction from ZK ice core  $\delta^{18}\text{O}$  record (ZK)  
 513 (b), the instrumental temperature record of the northern TP (ITNTP) (c), and global average  
 514 temperature (d). The decadal mean annual change rates were estimated using the  
 515 non-parametric LOESS regression model with a span of 0.4.



516  
 517  
 518  
 519  
 520  
 521  
 522

523 Table 1. Correlation coefficients and linear slopes between the  $\delta^{18}\text{O}$  values in the ZK ice core and  
 524 instrumental spring (March–May) and annual temperature from closest Gêrzê (1973–2008)  
 525 and Xainza stations (1961–2008), the averaged records of the two stations (1961–2008), and  
 526 the ITNTP series (1961–2008).

527

528

		Gêrzê		Xainza		Stations averaging		ITNTP
		March- May	Annual	March- May	Annual	March- May	Annual	Annual
Correlation coefficients	Annual	0.52 <sup>c</sup>	0.34 <sup>a</sup>	0.45 <sup>c</sup>	0.34 <sup>a</sup>	0.48 <sup>c</sup>	0.34 <sup>a</sup>	0.35 <sup>a</sup>
	5 year running average	0.63 <sup>c</sup>	0.53 <sup>c</sup>	0.73 <sup>c</sup>	0.60 <sup>c</sup>	0.73 <sup>c</sup>	0.60 <sup>c</sup>	0.61 <sup>c</sup>
	Slope							
	Annual	0.93 <sup>b</sup>	0.67 <sup>a</sup>	0.93 <sup>b</sup>	0.98 <sup>a</sup>	1.00 <sup>c</sup>	0.88 <sup>a</sup>	0.87 <sup>a</sup>
	5 year running average	0.87 <sup>c</sup>	0.76 <sup>c</sup>	1.54 <sup>c</sup>	1.32 <sup>c</sup>	1.37 <sup>c</sup>	1.18 <sup>c</sup>	0.40 <sup>c</sup>

529 <sup>a</sup>  $p < 0.05$ ; <sup>b</sup>  $p < 0.01$ ; <sup>c</sup>  $p < 0.001$ .

530

531 Table 2. Basic information of ice cores from the northern TP.

Ice core	Muztagata	ZK	Purogangri	Geladaindong	Malan
Latitude (N)	38°17'N	34°18'05.8"N	33°54'N	33°34'37.8"N	35°50'N
Longitude (E)	75°06'E	85°51'14.2"E	86°06'E	91°10'35.3"E	90°40'E
Altitude (m)	7010	6226	6200	5720	5680

532

533

534

535

536 Table 3. Correlation coefficients between the  $\delta^{18}\text{O}$  values in the ZK (1951–2008), Muztagata  
 537 (1955–2002), Puruogangri (1951–1998), Geladaindong (1951–2004) and Malan (1951–1999) ice  
 538 cores, and the regional  $\delta^{18}\text{O}$  values (1951–2002) averaged from ZK, Muztagata, Puruogangri and  
 539 Geladaindong ice cores. The values in bold are the correlation coefficients of annual values, and  
 540 the values in italic are the correlation coefficients of 5 year running average values

541

	ZK	Muztagata	Puruogangri	Geladaindong	Malan	Regional average
ZK		<b>0.26</b>	<b>0.14</b>	<b>-0.02</b>	<b>-0.27</b>	<b>0.57<sup>c</sup></b>
Muztagata	<i>0.68<sup>c</sup></i>		<b>0.09</b>	<b>0.04</b>	<b>-0.20</b>	<b>0.80<sup>c</sup></b>
Puruogangri	<i>0.46<sup>c</sup></i>	<i>0.28</i>		<b>-0.08</b>	<b>0.17</b>	<b>0.53<sup>c</sup></b>
Geladaindong	<i>-0.07</i>	<i>0.24</i>	<i>-0.12</i>		<b>0.05</b>	<b>0.30<sup>a</sup></b>
Malan	<i>-0.40<sup>b</sup></i>	<i>-0.33</i>	<i>0.14</i>	<i>0.18</i>		
Regional average	<i>0.79<sup>c</sup></i>	<i>0.95<sup>c</sup></i>	<i>0.54<sup>c</sup></i>	<i>0.31<sup>a</sup></i>		

542 <sup>a</sup>  $p < 0.05$ ; <sup>b</sup>  $p < 0.01$ ; <sup>c</sup>  $p < 0.001$ .

543